# NON-DESTRUCTIVE CHEMICAL ANALYSIS OF OLD SOUTH ARABIAN COINS, FOURTH CENTURY BCE TO THIRD CENTURY CE*

A. KIRFEL

*Steinmann Institut, Universität Bonn, Poppelsdorfer Schloss, D-53115 Bonn, Germany*

W. KOCKELMANN

*Science and Technology Facilities Council, Rutherford Appleton Laboratory, ISIS Facility, Didcot OX11 0QX, UK*

and P. YULE†

*Sprachen und Kulturen des Vorderen Orients-Semitistik, Ur- und Frühgeschichte und Vorderasiatische Archäologie, Universität Heidelberg, D-69117, Germany*

*Studies on Old South Arabian (OSA) coinage are rare and state-of-the-art materials analysis for them lags far behind that of ancient Greece and Rome. Understandably, numismatists responsible for preserving their collections discourage destructive analyses. We have selected coins of the aesthetically and technically developed Himyarite Royal Raydan series (early first to late second century CE), so-called Old and New Style Athenian Imitations, among others to provide a wide spectrum of information on OSA coinage. We used non-destructive neutron diffraction to ascertain the metal compositions and corrosion products. Density determinations using gas-pycnometry support these experiments. The results provide detailed information with regard to a small, apparently homogeneous, selection of 10 Himyarite period specimens and first insights into the actual and the original metal compositions of about 90 coins of the three main OSA numismatic groups. The analytical results make clear which OSA coins originally were struck and which ones were cast. The analyses provide not only detailed information concerning the manufacture of the selected representative coins, but also suffice to cast a shadow on the reliability of commonplace macro-optical classification, which proves often to be inaccurate.*

*KEYWORDS:* OLD SOUTH ARABIAN, NON-DESTRUCTIVE ANALYSIS, NEUTRON DIFFRACTION, SCYPHATE, ANGLE-DISPERSIVE MEASUREMENT

## INTRODUCTION

Under Greek influence, at the beginning of the fourth century BCE, Old South Arabian (OSA, centring on the Yemen) coinage emerged (fourth century BCE to third century CE: Sedov and Davidde 1998; Munro-Hay 2003; Huth 2011), and then waxed and waned successively during theSabaean, Qatabanian, Hadramitic and Himyarite periods, each with their characteristic motifs and styles. In 2004, Yule commenced systematic recording of OSA coinage in European collections while at the same time excavating Himyarite Zafar in the southern highlands of the Yemen. Himyar is the name of the tribal confederation and area in OSA that ultimately, for the first time,

unified Arabia as early as 270 CE. The collection of the State Ethnology Museum (SMVM) in Munich houses 419 different Old and New Style Athenian imitations, coins of the Himyarite Royal Raydan and the Sabaean Bucranion series, not to mention Byzantine, Roman, Hadhramitic and Axumite issues in gold, silver, copper and various alloys. Most of the collection was acquired in the Yemen in the 1980s, the vast majority by Dr Werner Daum (Berlin), who informed us that he also purchased a few at auction. Stuart Munro-Hay catalogued these coins for his handbook *Coinage of* Arabia Felix (2003). In a tolerant and thorough review, Hoover and Huth (2004) give credit where due and point out problems and pitfalls in this ambitious catalogue study. The evaluation of numerous OSA coins and their presentation in book form required more time than was available to that author, who unfortunately died without having seen his opus in printed form. This handbook has been described as a 'jungle of information' (ibid.). For example, Munro-Hay's disciplined treatment of coin types contrasts with the often lackadaisical and anarchic order of most of the illustrations. Assiduous numismatists need to make concordances in order to identify individual coins in the catalogue.

Although serious studies regarding coin production in general are plentiful (Grierson 1975; Göbl 1987; Moesta and Franke 1995), no one would contest that material analyses of OSA coins are virtually unknown. Most of the measurements reported here took place five at a time in 2004, when non-destructive analyses by neutron diffraction measurement were still few in number, and their potential with respect to the angle-dispersive and energy-dispersive modes was not fully assessed. In our still young archaeological subfield, material identifications—with few exceptions—are made with the naked eye. Munro-Hay barely mentions coin materials in his handbook. One exception (Munro-Hay 2003, 114) is as follows: 'Almost all of the coin units in the SMVM collection (92-316 751 nos. 283–291 and 92-316 847–851) are recorded as "billon" [Cu–Ag alloy, less than 50% Ag]; their appearance after cleaning resembles brass mixed with silver.'On p. 158, one reads, 'Some of each of the BYN types [py: in this collection] are recorded as debased silver'. Grave *et al.* (1996) contributed a material analysis of Eastern Arabian obols, drachms and tetradrachms. Such coins were analysed by means of proton-induced X-ray (PIXE) and gamma-ray emission (PIGME). For our experimental study, we selected typical OSA coins as well as atypical ones. The three main OSA coin groups selected include Old (Fig. 1, coin 1) and New Style Athenian Imitations (Fig. 1, coin 2) as well as the Himyarite Royal Raydan series (Fig. 1, coins 6 and 7).

Each such group of OSA coins is roughly dated. However, their absolute chronology is debatable (Munro-Hay 2003). Most (perhaps not all) would agree to use this group dating strategy instead of attempting gradual technical/stylistic development schemes such as the so-called art-historical method, because of the lack of chronological anchoring points.

Munro-Hay's subjective optical metal identifications deviate from those that we measured. Of 100 macro-optically, subjectively identified coin materials that he listed (Munro-Hay 2003, 207–8), 21 deviated from our physical test results. These include nos. 92-316 840, 841, 844, 850, 851, 858–863, 864, 870, 871, 872?, 878, 884, 886, 890 and 896, and 93-317 024. He also identifies some coins as cast forgeries—we comment on this below.

To the naked eye, most OSA coins—and therefore most of the coins in our selection—consist of silver and debased silver (less than 50% Ag). The peculiar concave–convex scyphate (Greek *trachy*) shape of numerous Himyarite Raydan series silver coins still inevitably raises the question of the method of striking and the reason behind it. This coin shape is best known from Byzantine medieval coins (Weber 2003–4, 28–31), but it is known from others (e.g., Celtic, Kushana) as well.

Before the question of the method of manufacture is addressed, we propose to non-destructively determine the metallurgical composition; that is, the phase abundance of Ag, Cu and

Figure 1 *Selected coins subjected to analysis: 1, Old Athenian Imitation; 2, New Athenian Imitation; 3, Bucranian Series; 4, Raydan Series, ancient forgery?; 5, Raydan Series, forgery; 6, Raydan Series; 7, Raydan Series, markedly scyphate; 8, Hadhrami cast copper coin. Scale 1.5:1.*

other metals. Moreover, does the silver content of the different issues remain constant over the years in different issues, or does it change with time as significant amounts of less precious metals were added? How does the silver content correspond with the stylistic/typological changes in numismatic history? How reliable are optical material identifications? In order to address these questions, we selected neutron diffraction as a method—it is a non-invasive analysis technique for metal objects (Kockelmann *et al.* 2006). In addition, a large number of the coins were also studied by gas-pycnometry in order to relate the observed experimental material density to the respective theoretical density calculated from the material composition as obtained from the diffraction analysis results.

NEUTRON DIFFRACTION

In the past decade, neutron diffraction has found increasing use in archaeological research, where it is not only a valuable tool for structure and phase analysis of an archaeological object, but can also help to shed light on its fabrication history (Kockelmann *et al.* 2000a, 2001, 2006). Compared to X-rays, the high penetration capability of neutrons particularly favours studies on ceramics and metal objects because: (i) they can be analysed non-destructively, without the need for special sample preparation; (ii) after penetrating coatings and/or corrosion layers, neutrons are well able to provide phase information from the bulk; and (iii) a neutron beam of typically

several mm² up to cm² in cross-section 'sees' the whole object, or at least a considerable portion of it, so that averaged and statistically representative information is obtained for one or several analysis points, as opposed to the usual metallographic single-spot analysis.

Basically, a diffraction experiment makes use of the coherent scattering by the periodic arrangement of scattering centres in crystalline matter, where it occurs only under material-specific diffraction angles given by the Bragg equation: $\lambda = 2d_{hkl}\sin\Theta$. In this equation, $\lambda$ is the wavelength, $\Theta$ is half the diffraction angle $2\Theta$, and $d_{hkl}$ is the distance between the equally spaced lattice planes with common orientation defined by the integer triple $hkl$.

For a polycrystalline sample with randomly oriented crystallites (e.g., powders and metals), the diffraction pattern plots 'intensity versus diffraction angle'. Thus, in this angle-dispersive mode using monochromatic radiation ($\lambda$ = const.), one obtains diffraction peaks as a function of the diffraction angle. In the energy-dispersive case using 'white' radiation with a broad range of wavelengths (energies), scattering at a fixed $2\Theta$ gives rise to peaks whenever a combination of wavelength and $d_{hkl}$ meets Bragg's law. Therefore, the diffraction pattern displays intensities versus $d$-spacings. While the Bragg equation accounts only for the geometrical aspect—in other words, the peak positions—the intensities of the individual peaks depend on the scattering density distribution in the unit cell of the structure. As a rule of thumb, metal structures exhibit small unit cells with high symmetry, yielding diffraction patterns with few, well-resolved peaks.

In a multi-phase sample, the individual patterns of the different crystalline phases are superposed, each weighted with the component's abundance. The resulting total diffraction pattern can be analysed, first to identify, and second to quantify, the phase mixture. For coins, this applies to the different metals or alloys and their abundances, but also to possible corrosion products such as oxides and chlorides. Moreover, the metal peak intensities also reflect possible deviations from a random orientation distribution of the crystallites and, similarly, the peak profile shapes can reflect details of the sample's microstructure; for example, crystallite sizes or strain. Thus, diffraction data can also yield information about texture and microstructure, which may relate to the mechanical and thermodynamic history of the object. The first step in each analysis is to compare the observed peak positions with those of single-phase patterns stored in databases in order to determine the combination of phases present in the sample. Once the individual phases are identified by means of search-match routines—that is, qualitative analysis is achieved—quantitative phase analysis assesses the relative amount of each phase, usually in weight per cent. This is done under the assumptions that (i) each phase exhibits a unique set of diffraction peaks, and (ii) the phase-specific intensities are proportional to the phase content. The so-called full-pattern Rietveld analysis (Rietveld 1967, 1969; Young 1993) allows the least-squares refinement of phase-specific parameters such as the scale factor, the lattice constants and/or structure parameters, along with experiment-specific peak profile and background parameters. Generally, the phase abundances are given in weight fractions, $w_p$, which can be transformed into relative phase fractions—that is, the percentages of the different phases in the mixture—according to

$$S_p = \left[ w_P / \left( Z_P * MW_P V_P \right) \right] / \left[ \Sigma w_j \left( Z_j * MW_j V_j \right) \right], \tag{1}$$

where $MW_p$ is the molecular mass of the formula unit, and $Z_p$ is the number of times the chemical formula is contained in the unit cell with volume $V_p$. Then, the total theoretical density of the sample follows from $\rho_{tot} = \Sigma S_p \rho_p$, where $\rho_p$, the density of the $p$th crystalline phase, can be taken from a database or from the literature.

*A. Kirfel, W. Kockelmann and P. Yule*

The so-called estimated standard deviation (e.s.d.) obtained from the Rietveld fits is about 0.1 wt% for the energy-dispersive data, and 0.5 wt% for the angle-dispersive data. These are uncertainties solely based on counting statistics, concerning the reproducibility of the fit results. The estimated uncertainty of the weight fraction is larger; that is, for Cu, Ag, $Cu_2O$ and chloride phases, of the order of 0.5 wt% and 1 wt%, respectively, for the energy- and angle-dispersive results, as obtained from measurements on test samples with known compositions. The uncertainty and detection limit of Pb are about 1%.

In the present study, full-pattern analysis and both diffraction modes were brought to bear in order to characterize:
• a batch of 10 Himyarite, apparently hardly corroded, silver coins (hereafter addressed as SEL1) with respect to fine details of composition and strain in correlation with their shapes and appearances by means of energy-dispersive data; and
• a batch of 89 coins (SEL2) from the same collection of more varied, mostly OSA origin, coins, often seemingly similar in composition, but with different degrees of corrosion, with respect to their composition (compared to visual classification) using angle-dispersive data.

### EXPERIMENTAL

The experimental densities, $\rho_{exp}$, of a subset of 63 coins were determined using a Micromeritics 1305 Multivolume Pycnometer. This instrument works by He-gas displacement and measures the volume of a solid object, be it of irregular or regular shape, in one piece or as powder. The cylindrical sample chamber is first charged to a gas pressure of about 1.5 bar. Subsequent expansion of this gas charge into a second precisely measured volume filled with gas of the same temperature and at 1 bar results in a second pressure, which becomes increasingly smaller for larger samples. Then, the application of mass balance equations for the gas permits calculation of the sample volume, provided that the volumes of the empty chambers as well as the pressure drop ratio upon expansion are known. The instrument was calibrated on the 5 cm$^3$ range using as standard volume the precision ball supplied with the instrument (accuracy/reproducibility: 10.1% (0.005 cm$^3$)).

After careful tests with coin replicas of pure Ag and Cu, all objects small enough to fit in the sample chamber were measured in order to cross-check the phase analyses (within error limits, $\rho_{exp}$ must not exceed $\rho_{theor}$) and/or to use the positive density differences $\Delta\rho = \rho_{theor} - \rho_{exp}$ as an indicator of the degree of internal corrosion.

The neutron measurements were performed in 2005 and 2006 at the pulsed neutron spallation source ISIS, at the Rutherford Appleton Laboratory (UK), and at a continuous neutron source, the DIDO reactor, FRJ-2 Juelich (Germany), where the former Mineralogical Institute of the University of Bonn (Germany) maintained the experimental stations ROTAX and SV7a,b, respectively, both devoted to internal and external user programmes of materials research.

The angle-dispersive measurements were carried out on the powder diffractometer SV7a (Schäfer *et al.* 1997; Kirfel *et al.* 2006). Using a fixed wavelength of 1.0959 Å (Ni-(220) monochromator), a batch of 89 coins was inspected. Each coin was held in place with a boron carbide rubber sample holder, and mounted on a goniometer head with the coin standing upright and parallel to the Eulerian cradle's $\chi$-circle, so that the coin, as a 'convex mirror', reflected the incident radiation into the detector. With a beam cross-section of 11 mm width and 35 mm height, each diagram was recorded in steps of 0.1° for a $2\Theta$ range from 4 to 89°. The scan time was 4 h per coin.

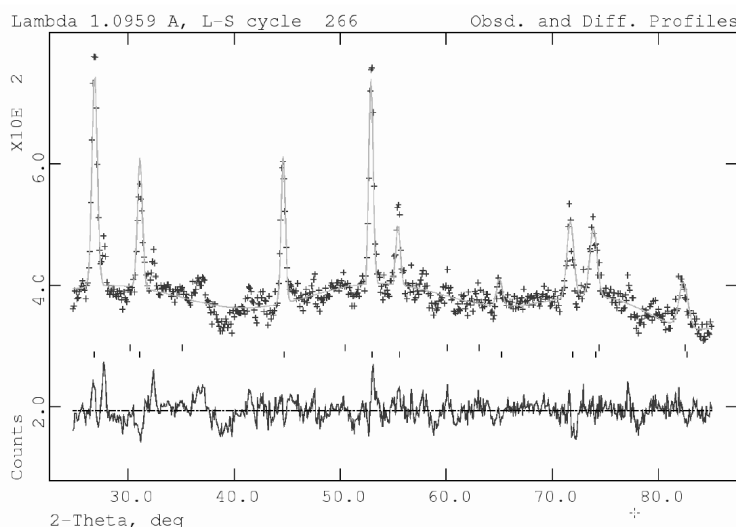*Non-destructive chemical analysis of Old South Arabian coins*



Figure 2 *The diffraction pattern obtained in angle-dispersive mode at SV7a on coin no. 063.*

Data processing was performed by full-pattern Rietveld refinements (FULLPROF: Rodriguez-Carvajal 1993) after identification of the phases present. These were Ag (Ag/Au assumed for golden coins), Cu, Pb and the corrosion products AgCl and $Cu_2O$. A typical example of an angle-dispersive diffraction pattern and fit curve is depicted in Figure 2. The resulting abundances given in weight per cent were recalculated as relative phase fractions (%), which in turn served to calculate the theoretical density $\rho_{theor} = \rho_{calc}$ of each sample material as the sum of the phase fraction weighted densities of the individual phases.

Coins in SEL 1 were also inspected for crystallographic texture effects; that is, preferred orientations of crystallites that are produced by mechanical treatment. For a coin minted by striking or deep-drawing (a metal blank radially drawn into a forming die by means of a punch), the texture analysis should show regular, smooth intensity variations when diagrams are recorded at systematically varied sample orientations with respect to the incident radiation. For a cast coin, on the other hand, there are no such regular preferred orientations of the crystallites, so that a corresponding sequence of diagrams shows no, or at best irregular, intensity variations of a Bragg reflection when the sample is rotated in the neutron beam. Thus, a sufficiently large number of diagrams transformed into a so-called pole-figure, which illustrates the distribution of crystallite orientations, can provide information about the fabrication of a coin (Kockelmann *et al.* 2006). Due to time limits, complete texture analyses could not be performed for all coins. However, partial texture scans were performed for a limited range of sample reorientations on the texture diffractometer SV7b with a neutron wavelength of 2.332 Å, using a pyrolytic graphite monochromator (PG(002)). The beam cross-section was 30 x 30 $mm^2$. The time spent for one coin was about 24 h.

The energy-dispersive measurements were carried out on the time-of-flight (TOF) neutron spectrometer ROTAX installed at ISIS (Kockelmann *et al.* 2000b). On ROTAX, neutron wavelengths in the range between 0.5 and 5 Å relate to neutron velocities ($v$) between 8000 and 800 m $s^{-1}$, respectively. Given a flight path from source to detector, measurement of the flight time of a neutron determines its velocity and energy, which via Bragg's equation correlates with a crystallographic *d*-spacing. In order to be 'neutron efficient', multiple detector devices or
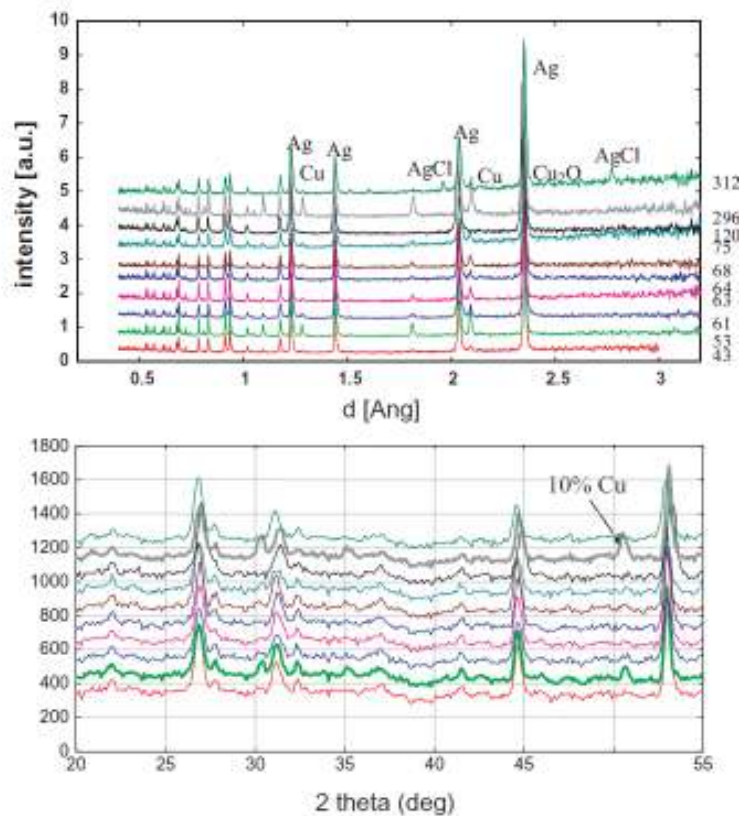
*A. Kirfel, W. Kockelmann and P. Yule*



Figure 3 *Selection SEL1: a comparison of the 10 diffraction patterns obtained in energy-dispersive mode on ROTAX (ISIS) and in angle-dispersive mode at SV7a (below).With similar data collection times, the advantage of TOF measuring multi-detector equipment is evident.*

position-sensitive detector banks at different angles are employed on energy-dispersive neutron instruments, so that energy-dispersive diffraction patterns are simultaneously recorded for a large number of diffraction angles. This information is then electronically processed and finally focused into a single *I* versus *d*-spacing pattern, one per detector bank. The *d*-spacing resolution is the better, the larger the $2\Theta$ angle of the detector bank. Thus, small *d*-spacings are best studied by a detector (bank) in backscattering position. The TOF experiments on ROTAX were carried out on 10 specially selected silver coins (SEL1) considered representative for the Himyarite Raydan Series. Since the coins are not moved during data collection, they could be placed in vanadium sachets suspended in the beam, with the convex coin sides facing the beam. The vanadium holder does not produce significant Bragg peaks. Owing to the much larger neutron flux provided by the 'white radiation' as compared to the monochromatic radiation at SV7, data collection times between 1 and 2 h were sufficient to obtain satisfactory diffraction data. A comparison of the spectra measured at ISIS with those produced on the same coins at FRJ-2 is made in Figure 3, which for both scattering modes depicts all 10 spectra in order to emphasize common features and differences.

*Non-destructive chemical analysis of Old South Arabian coins*

Table 1 *Selection SEL1: phase fractions [%] and strain parameter* e = D*d/d* = G*/DIFC (DIFC = 6605.3 for the backscattering detector bank); SK = (height - thickness)/diameter; Himyarite Royal Raydan Series coins, analysed at the ISIS Facility, Rutherford Appleton Laboratory, UK; ROTAX TOF-diffractometer; energy-dispersive measurements for phase and strain analysis*

| museum inv. no. | Ag (%) | Cu (%) | Cu$_2$O (%) | AgCl (%) | SK | ε x10$^4$ |
|---|---|---|---|---|---|---|
| 92-316 296 | 80.3 | 19.5 | 0.2 | 0.0 | 0.062 | 15.4 |
| 92-316 312 (1) | 96.3 | 0.8 | 1.7 | 1.1 | 0.068 | 41.9 |
| 92-316 312 (2) | 96.1 | 0.9 | 1.8 | 1.1 | 0.068 | 41.0 |
| 92-316 751 043 | 96.5 | 3.4 | 0.1 | 0.0 | 0.195 | 24.4 |
| 92-316 751 053 | 85.7 | 14.1 | 0.1 | 0.0 | 0.173 | 39.2 |
| 92-316 751 061 | 94.6 | 5.0 | 0.25 | 0.1 | 0.235 | 41.3 |
| 92-316 751 063 | 94,6 | 5.0 | 0.25 | 0.1 | 0.133 | 12.0 |
| 92-316 751 064 | 96.8 | 2.9 | 0.3 | 0.0 | 0.199 | 29.5 |
| 92-316 751 068 | 92.8 | 6.8 | 0.4 | 0.0 | 0.159 | 20.1 |
| 92-316 751 075 (1) | 94.7 | 5.3 | 0.0 | 0.0 | 0.162 | 43.1 |
| 92-316 751 075 (2) | 95.0 | 4.7 | 0.3 | 0.0 | 0.162 | 41.3 |
| 92-316 751 120 | 99.7 | 0.0 | 0.3 | 0.0 | 0.112 | 44.5 |

Rietveld fits of the backscattered diffraction data were carried out using the program package GSAS (Larson and von Dreele 2004). The refinements included the adjustment of a strain parameter Γ, which can be converted into $\varepsilon = \Gamma/DIFC = \Delta d/d$, where *DIFC* is an instrument parameter as defined in the GSAS manual. The parameter e accounts for reflection broadening due to internal strains, which are related to mechanical forces exerted on the coin during manufacture.

MATERIAL ANALYSIS RESULTS

*Selection of 10 coins (SEL1)*

The phase fractions of 10 coins of the Himyarite Royal Raydan Series given in Table 1 corroborated the visual impression of little corroded silver-rich objects. The agreement of the results obtained from two coins that were measured twice (nos. 075 and 312) illustrates the reproducibility and reliability of the derived compositions. It should be noted that the neutron diffraction method does not distinguish between phases on the surface or in the interior of a coin.

Although the selected specimens appeared to make up a fairly homogeneous set, closer inspection of the identified phases, their abundances, their strain parameters and the 'convexities' ((height minus thickness)/diameter ratios; see Table 1) revealed some interesting differences:

(i) Eight of the 10 coins are made of more than 92.8% silver, the remaining material consisting of copper and varying amounts of the corrosion products AgCl and Cu$_2$O, with phase fractions typically below 0.4%. Coin no. 312 deviates from this pattern, as it exhibits significantly more corrosion, indicated by 1.7–1.8% cuprite and 1.1% silver chloride.

(ii) Two objects, nos. 053 and 296 (Fig. 1, coin 5), contain less silver; that is, 85.7 and 80.3%, respectively. Being hardly corroded, the remaining fractions are 14.1 and 19.5% copper. Thus, on the basis of the mere phase contents, one could speculate that these coins stem from a different workshop batch or were made at different times. However, these two coins are significantly
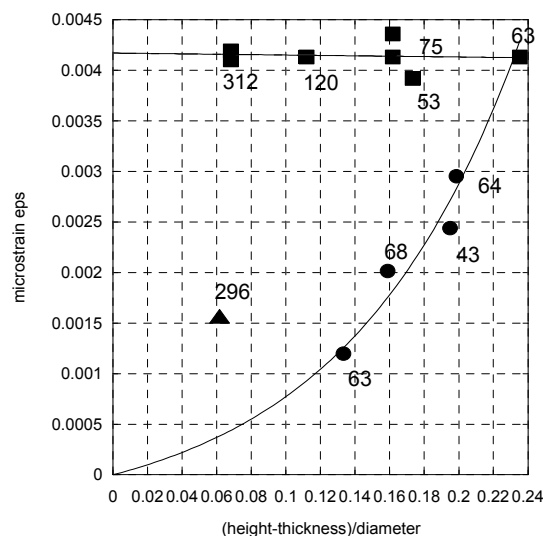
*A. Kirfel, W. Kockelmann and P. Yule*



Figure 4 *Selection SEL1: microstrain parameter ε versus the 'convexity' of the scyphate coins (for details, see the text).*

different in terms of their strain parameters and shapes. While no. 053 belongs to the most scyphate items, no. 296 is rather flat.

(iii) In this context, it is interesting to consider Figure 4, which plots the strain parameter $\varepsilon$ against the geometrical ratio $SK$ = (height - thickness)/diameter representing the convexity of a coin. If one assumes that e increases with increasing $SK$, four coins (nos. 043, 063, 064 and 068) conform, but no. 296 does not. As its surface also showed cavities or surface bubbles, it can be inferred that no. 296 does not fit into the SEL1 set, because it seems that it was cast (see below). It is also intriguing that five of the 10 coins, among them no. 053, seem to constitute a separate group with almost equally large e-values that are independent of the shape. This finding implies that after their fabrication, the microstrain introduced by striking may have been 'overwritten' by subsequently introduced strains; for example, by quenching the coin (after hot minting).

In order to confirm suspicion of coin no. 296 (Fig. 1, coin 7) as a forgery, following the identification of Munro-Hay (2003, 207), additional texture measurements were performed on this coin, and compared with the texture of no. 061. Figure 5 shows cascades of diffraction patterns recorded for equally spaced coin orientations. Comparing, for example, the evolution of the intensity of the strong Ag reflection, no. 220, clearly shows that this is smooth and regular in case of no. 061, whereas it is irregular for no. 296. The latter finding, typical for a cast item, underlines the suspicion that no. 296 was not produced in the standard way; that is, by striking.

It should be noted that the neutron diffraction method can distinguish a copper alloy phase from pure copper only by a shift of the lattice constant of the unit cell. The question of whether or not the copper phase accommodates Sn or other alloying elements cannot be answered on the basis of the given data. It is likely that the copper contains trace elements that are unrecognizable by the diffraction method. However, upper limits can be given as 'Sn equivalent' fractions, which are lower than 1% for the coins in Table 1. One exception is coin no. 296, which has an increased lattice parameter indicating a Sn-equivalent fraction of 3%.
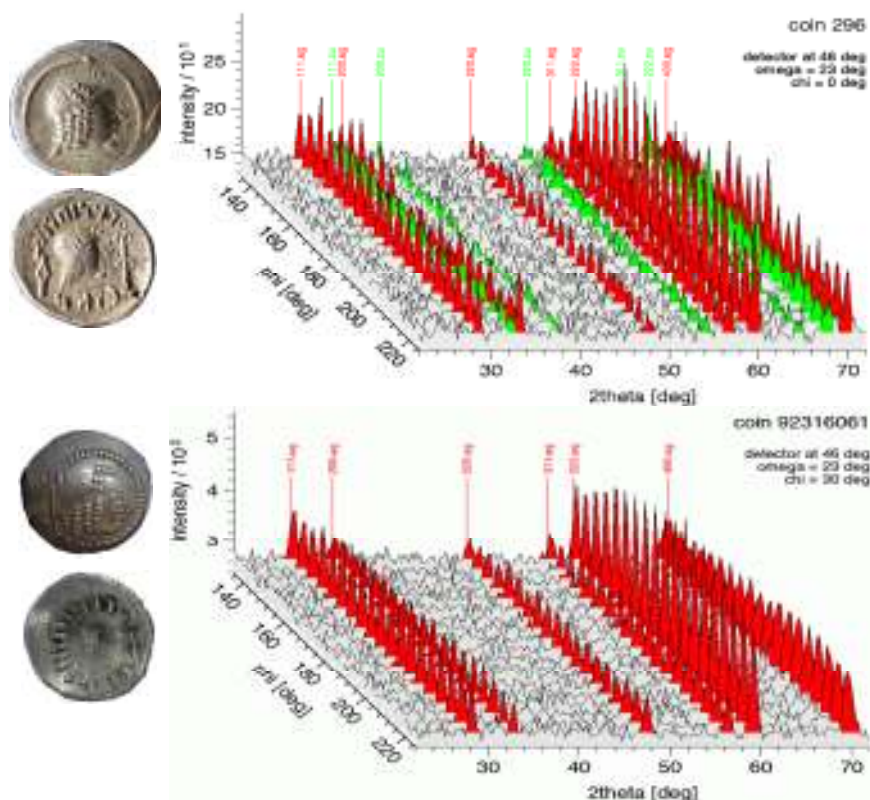
*Non-destructive chemical analysis of Old South Arabian coins*



Figure 5 *Angle-dispersive texture measurements performed on SV7b: coin no. 296 (above) and no. 061 (below). Note the smooth intensity changes upon rotation for no. 061 compared to the irregular changes exhibited by no. 296, suspected to be a cast coin.*

*Selection of 89 coins (SEL2)*

Coins in selection SEL2 were studied by angle-dispersive neutron diffraction. Their identifications, classifications, relative phase fractions and calculated densities are compiled in Table 2. Where available, $\rho_{exp}$ is also given for comparison. The metals identified in SEL2 were Ag, Cu and Pb, and the corrosion products found were AgCl and $Cu_2O$. For the golden coins, Au had, of course, to be considered as a possible phase. The crystallographic phases were used to model the observed diffraction patterns by Rietveld refinements. Since Ag and Au are isotypic, with very similar lattice parameters $a_0$, and since the two metals form solid solutions without significant changes in $a_0$, the Au/Ag contents of the few optically golden coins were deduced from the experimental density determinations.

The question of whether or not the copper phase accommodates Sn or other alloying elements cannot be answered on the basis of the given data. Shifts of the lattice constants of the copper phase are small for the studied coins. Due to the low counting statistics, we considered the quality of the diffraction data insufficiently good for a reliable determination of $a_0$. XRF would only be able to detect elements on the surface of coins. The characteristic compositions of the three most populated groups, HIM, IOA and INA (see also Fig. 6), can be described as follows. The HIM coins consist of Ag and Cu with Ag/(Ag + Cu)

*A. Kirfel, W. Kockelmann and P. Yule*

Table 2  Selection SEL2: phase fractions and densities of coins, sorted by coin group; analysed at the DIDO reactor FRJ-2 Juelich, Germany; SV7a-diffractometer; angle-dispersive measurements for phase analysis; the phase fraction values in the left-hand part of the table are measured, and those on the right are calculated as indicating the phase fractions before corrosion

| Inv. no. | Ag (frac%) | AgCl | Au | Cu | Cu₂O | Pb | Cat.* | impr† | ρcalc (g cm⁻³) | ρexp (g cm⁻³) | Remarks‡ | Ag₀ | Cu₀ | Pb₀ |
|---|---|---|---|---|---|---|---|---|---|---|---|---|---|---|
| 92-316816 |  |  |  | 95 |  | 5 | Ptol | Br | 9.58 |  |  |  | 95 | 5 |
| 92-316817 | 25 |  |  | 75 |  |  | Rom | Ag | 9.31 | 9.46 |  | 25 | 75 |  |
| 92-316818 |  |  | 100 |  |  |  | Byz | Au | 19.32 | 19.40 |  |  |  |  |
| 92-316819 | 14 |  | 86 |  |  |  | Byz | Au |  | 18.65 | a.d. |  |  |  |
| 92-316820 |  |  | 100 |  |  |  | Axu | Au | 19.32 | 19.37 |  |  |  |  |
| 92-316821 | 7 |  | 93 |  |  |  | Axu | Au |  | 18.96 | a.d. |  |  |  |
| 92-316822 | 41.5 |  | 58.5 |  |  |  | Axu | Au |  | 18.86 | a.d. |  |  |  |
| 92-316823 | 98 |  | 2 |  |  |  | Axu | Ag | 10.69 | 10.70 |  |  |  |  |
| 92-316824 | 99.4 | 0.6 |  |  |  |  | INA | Ag | 10.46 | 10.13 |  | 100 |  |  |
| 92-316825 | 99.4 | 0.6 |  |  |  |  | INA | Ag | 10.46 | 10.20 |  | 100 |  |  |
| 92-316826 | 91 | 9 | 9 |  |  |  | INA | Ag | 10.10 |  |  | 100 |  |  |
| 92-316827 | 96.5 | 3.5 |  |  |  |  | INA | Ag | 10.34 | 9.21 |  | 100 |  |  |
| 92-316828 | 65 | 35 |  |  |  |  | INA | Ag | 9.00 | 7.76 |  | 100 |  |  |
| 92-316829 | 92 | 8 |  |  |  |  | INA | Ag | 10.15 | 9.43 |  | 100 |  |  |
| 92-316830 | 99 | 1 |  |  |  |  | INA | Ag | 10.44 | 9.61 |  | 100 |  |  |
| 92-316831 | 100 |  |  |  |  |  | INA | Ag | 10.49 | 10.49 |  | 100 |  |  |
| 92-316832 | 97 | 3 |  |  |  |  | INA | Ag | 10.37 | 10.43 |  | 100 |  |  |
| 92-316833 | 96.5 | 3.5 |  |  |  |  | INA | Ag | 10.34 | 10.11 |  | 100 |  |  |
| 92-316334 | 89 | 11 |  |  |  |  | INA | Ag | 10.02 | 10.45 |  | 100 |  |  |
| 92-316835 | 65 | 35 |  |  |  |  | INA | Ag | 9.00 | 8.98 |  | 100 |  |  |
| 92-316836 | 97 | 3 |  |  |  |  | INA | Ag | 10.37 | 9.80 |  | 100 |  |  |
| 92-316837 | 100 |  |  |  |  |  | INA | Ag | 10.49 | 10.35 |  | 100 |  |  |
| 92-316838 | 78.5 |  |  | 21.5 |  |  | INA | Ag | 10.15 | 10.15 |  | 78.5 | 21.5 |  |
| 92-316839 | 95 |  |  | 5 |  |  | INA | Ag | 10.41 | 10.41 |  | 95 | 5 |  |
| 92-316840 | 98 |  |  |  |  | 2 | IOA | Br | 10.71 |  |  | 98 |  | 2 |
| 92-316841 | 100 |  |  |  |  |  | IOA | Br | 10.49 | 10.23 |  | 100 |  |  |
| 92-316842 | 52.5 |  |  | 45 |  | 2.5 | IOA | Br | 10.10 | 10.15 |  | 52.5 | 45 | 2.5 |
| 92-316843 | 26.8 |  |  | 71.7 |  | 1.5 | IOA | Cu | 9.54 |  |  | 26.8 | 71.7 | 1.5 |
| 92-316844 | 45 |  |  | 55 |  |  | BUC | Ag | 9.63 | 9.99 |  | 45 | 55 |  |
| 92-316845 | 35 |  |  | 65 |  |  | BUC | Ag | 9.47 | 9.65 |  | 35 | 65 |  |
| 92-316846 | 91 |  |  | 7 |  | 2 | BUC | Ag | 10.59 |  |  | 91 | 7 | 2 |
| 92-316847 | 62 |  |  | 38 |  |  | IOA | Bi | 9.89 |  |  | 62 | 38 |  |
| 92-316848 | 63.5 |  |  | 36.5 |  |  | IOA | Bi | 9.92 | 9.60 |  | 63.5 | 36.5 |  |
| 92-316849 | 73.5 |  |  | 24.5 |  | 2 | IOA | Ag | 10.36 |  |  | 73.5 | 24.5 | 2 |

| Sample | Mint | Element | Ag | Cu | (tr) | V1 | V2 | Other |
|---|---|---|---|---|---|---|---|---|
| 92-316850 | IOA | Ag | 90.5 | 7.5 | 2 | 10.62 | 8.35 | |
| 92-316851 | IOA | Cu | 91 | 9 | | 10.34 | 9.61 | |
| 92-316852 | IOA | Bi | 47.5 | 52.5 | | 9.67 | 9.88 | |
| 92-316853 | IOA | Bi | 99 | 1 | | 10.64 | 9.39 | |
| 92-316854 | IOA | Bi | 99.7 | 0.3 | | 10.52 | 8.79 | |
| 92-316855 | IOA | Bi | 71 | 27.5 | 1.5 | 10.21 | 8.99 | |
| 92-316856 | IOA | Bi | 94.3 | 5.5 | 0.3 | 10.15 | 8.72 | |
| 92-316857 | IOA | Bi | 99.7 | | 0.3 | 10.53 | 9.79 | |
| 92-316858 | IOA | Bi | 99.7 | | 0.3 | 10.34 | 8.95 | |
| 92-316859 | Him | Ag | 91 | 9 | | 10.41 | 9.79 | |
| 92-316860 | Him | Ag | 95 | 5 | | 10.02 | 10.19 | |
| 92-316861 | Him | Ag | 70 | 30 | | 10.47 | 9.54 | |
| 92-316862 | Him | Ag | 84 | 14 | 2 | 10.50 | 7.74 | |
| 92-316863 | Him | Ag | 76.4 | 20.8 | 2.8 | 8.25 | | 7 |
| 92-316864 | Him | Ag | 15.3 | 84.7 | | 10.95 | 9.08 | |
| 92-316865 | Him | Ag | 78.7 | 15.4 | 5.8 | 10.75 | 9.44 | |
| 92-316866 | Him | Ag | 78.3 | 17.2 | 4.5 | 10.24 | 9.48 | 32.2 |
| 92-316867 | Him | Ag | 84.5 | 15.5 | | 10.31 | | |
| 92-316868 | Him | Ag | 88.5 | 11.5 | | 9.19 | 9.30 | |
| 92-316869 | Him | Ag | 17.5 | 82.5 | | 9.69 | 9.10 | |
| 92-316870 | Him | Ag | 47.5 | 52.5 | | 9.22 | 9.61 | |
| 92-316871 | Him | Ag | 19.5 | 80.5 | | 9.99 | 8.55 | |
| 92-316872 | Him | Ag | 68 | 32 | | 9.15 | 9.21 | |
| 92-316873 | Him | Ag | 15 | 85 | | 9.35 | 9.00 | |
| 92-316874 | Him | Ag | 27.5 | 72.5 | | 9.05 | 8.09 | |
| 92-316875 | Him | Ag | 8 | 92 | | 9.50 | 9.21 | |
| 92-316876 | Him | Ag | 37 | 63 | | 9.48 | 9.49 | |
| 92-316877 | Him | Ag | 35.5 | 64.5 | | 9.78 | 8.91 | |
| 92-316878 | Him | Ag | 55 | 45 | | 9.35 | 7.78 | |
| 92-316879 | Him | Ag | 27.5 | 72.5 | | 9.35 | 8.19 | |
| 92-316880 | Him | Ag | 27.5 | 72.5 | | 9.22 | 6.80 | |
| 92-316881 | Him | Ag | 19.5 | 80.5 | | 9.40 | 10.16 | |
| 92-316882 | Him | Ag | 30.5 | 69.5 | | 9.06 | 9.43 | |
| 92-316883 | Him | Ag | 9 | 91 | | 10.78 | 9.15 | |
| 92-316884 | Him | Ag | 97 | 0 | 3 | 8.92 | 9.33 | 3 |
| 92-316885 | Him | Ag | | 100 | | 9.32 | 6.15 | |
| 92-316886 | Him | Ag | 47.5 | 52.5 | | 10.24 | | 12.5 |
| 92-316887 | Him | Ag | 84.5 | 15.5 | | 10.15 | | |
| 92-316888 | Him | Ag | 78.5 | 21.5 | | 10.31 | | |
| 92-316889 | Him | Ag | 88.5 | 11.5 | | 9.29 | | |
| 92-316890 | Him | Ag | 23.5 | 76.5 | | 9.16 | | |
| 92-316891 | Him | Cu | 38 | 62 | | | | 12 |

*A. Kirfel, W. Kockelmann and P. Yule*

Table 2   *(Continued)*

| Inv. no. | Ag (frac%) | AgCl | Au | Cu | $Cu_2O$ | Pb | Cat.* | impr† | $\rho_{calc}$ (g cm$^{-3}$) | $\rho_{exp}$ (g cm$^{-3}$) | Remarks‡ | $Ag_0$ | $Cu_0$ | $Pb_0$ |
|---|---|---|---|---|---|---|---|---|---|---|---|---|---|---|
| 92-316 892 | | | | 80.5 | 19.5 | | Him | Cu | 8.37 | 7.72 | | | 100 | |
| 92-316 893 | | | | 58 | 40.5 | 1.5 | Him | Cu | 7.97 | | | | 98.5 | 1.5 |
| 92-316 894 | | | | 89.5 | 10.5 | | Him | Cu | 8.62 | | | | 100 | |
| 92-316 895 | | | | 65 | 35 | | Him | Cu | 7.94 | | | | 100 | |
| 92-316 896 | 100 | | | | | | Him | Ag | 10.49 | | | 100 | | |
| 92-316 897 | | | | | | 100 | Isl | Ag | 22.49 | | | | | 100 |
| 93-317 022 | 77 | | | 97.5 | | 2.5 | Had | Cu | 9.25 | | | | 97.5 | 2.5 |
| 93-317 023 | 97 | | | 15 | 8 | | IOA | Br | 9.89 | | | 77 | 23 | |
| 93-317 024 | | 3 | | | | | IOA | Br | 10.37 | | | 100 | | |
| 93-317 485 | | | | 97.5 | | 2.5 | Had | Cu | 9.27 | | | | 97.5 | 2.5 |
| 93-317 486 | 91 | | | 9 | | | IOA | Br | 10.37 | | | 91 | 9 | |
| 93-317 487 | 15.5 | | | 67.5 | 17 | | Him | Ag | 8.69 | | | 15.5 | 84.5 | |
| 93-317 488 | 88.5 | | | 11.5 | | | Him | Ag | 10.31 | 9.89 | | 88.5 | 11.5 | |
| 93-317 489 | | | | | | | Him | Ag | | | | | | |
| 93-317 490 | | | | | | | Him | Ag | | | | | | |
| 93-317 491 | | | | | | | Him | Ag | | | | | | |
| 93-317 492 | | | | | | | Him | Ag | | | | | | |
| 93-317 740 | 88.5 | | | 11.5 | | | Him | Ag | 10.31 | | | 88.5 | 11.5 | |

*Abbreviations: Axu = axumite, Buc = Bucranian Series, Byz = Byzantine, Had = Hadrani, Him = Himyarite Raydan Series, INA = New Athenian Imitation, IOA = Old Athenian Imitation, Isl = Islamic period, Ptol = Ptolemaic.

†The abbreviation 'impr' refers to optical identification.

‡a.d. = assumed from experimental density.

*Non-destructive chemical analysis of Old South Arabian coins*
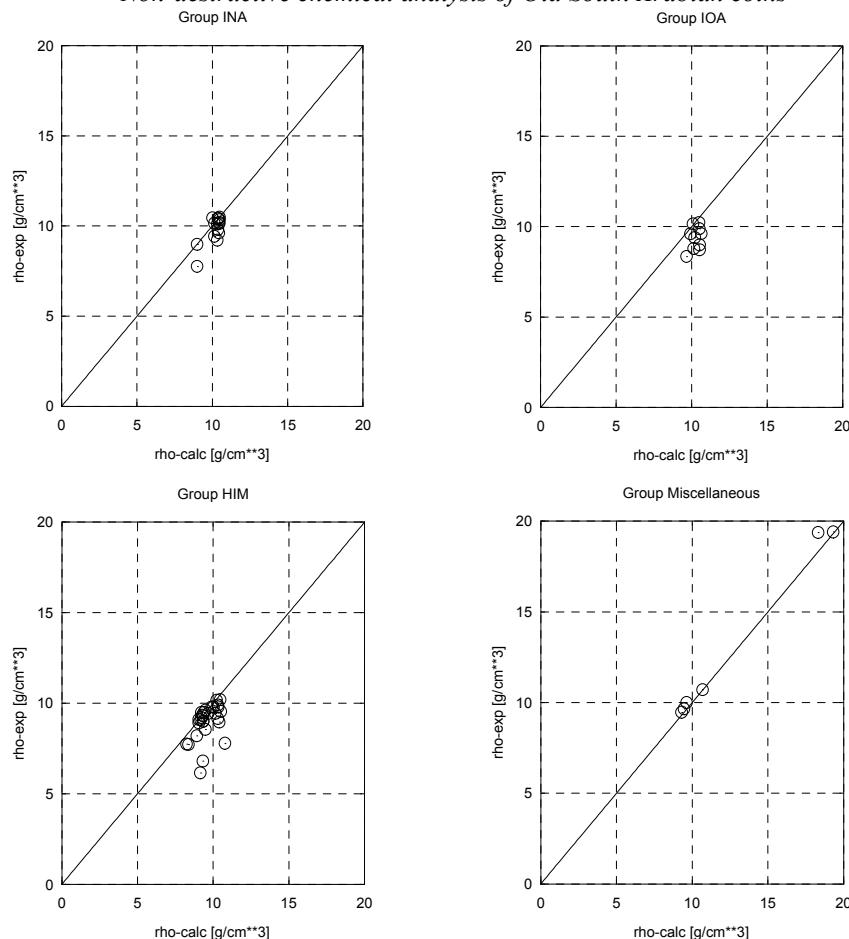


Figure 6 *The experimental density, ρ_exp, versus the theoretical density, ρ_calc, calculated from refined phase fractions (63 coins), groups New and Old Athenian Imitations, Himyarite and selected miscellaneous coins.*

ratios between 1.0 and 0.0. Corrosion resulted in up to 40% of the oxidation product $Cu_2O$. For the IOA group, the smallest Ag fraction is about 27% and corrosion products were not detected. Common to both groups are coins which possess small fractions of lead, up to 6% (no. 865), but such admixtures of lead do not seem to follow a system. Clearly distinguishable from both HIM and IOA is the group of coins classified as INA. All coins of the latter group except one (no. 838) were apparently made of silver and exhibit varying degrees of corrosion; that is, of AgCl of up to 20%. Only coin no. 838 of the INA group was found to contain copper, so that it may be a case where the phase analysis can stimulate reclassification of the coin. All in all, considering the material composition, one can state that the HIM and IOA coins were made from Ag–Cu mixtures, occasionally including some Pb. The compositions are similar and differ only with respect to the $Cu_2O$ corrosion; they show no AgCl corrosion. Clearly different is the group INA, made of pure Ag and exhibiting considerable amounts of AgCl corrosion.

The diffraction results obtained can be complemented and underlined by considering the results of the density determinations. Figure 6 plots all determined $\rho_{exp}$ values against $\rho_{calc}$ as

obtained from the refined phase fractions. The results are separate for the groups INA, HIM, IOA and some miscellaneous coins. If a coin was uncorroded and had no internal micropores and/or scissures, its symbol in Figure 6 should be on or close to the diagonal $\rho_{exp} \cong \rho_{calc}$ line. Positive deviations, $\rho_{exp} > \rho_{calc}$, should only occur within the experimental uncertainty limits. The fact that Figure 6 conforms with this constraint validates the diffraction results. On the other hand, negative deviations are always possible if corrosion has taken place, according to the reactions $2Cu + O \rightarrow Cu_2O$ and $Ag + Cl \rightarrow AgCl$. While the copper oxidation can happen almost any time and everywhere, provided that oxygen is available, the second reaction requires the presence of Cl (which also acts as catalyst for the first reaction). As an inspection of Table 2 shows, the presence of Cl applies to the species of group INA, whereas all other samples of SEL2 exhibit solely copper and small lead admixtures. Coin no. 897, consisting of pure lead, was apparently wrongly classified. Obviously, all groups except the last contain more or less corroded members with $\rho_{exp} < \rho_{calc}$, except for one with $\rho_{exp} > \rho_{calc}$. This finding implies that the discrepancies between $\rho_{exp}$ and $\rho_{calc}$ are primarily due to corrosion. Thus, the density determinations contribute additional information supporting the interpretation of the obtained phase fractions, and hence degrees of corrosion.

Also interesting in this context is Figure 7 (a), which depicts the copper fractions compared to silver ones. The elliptic symbols consider all coins, the open rectangles referring to those that are Himyarite; that is, belong to group HIM. Symbols on the borders indicate coins made of pure Ag or Cu, respectively, which are either corroded and/or contain additional metals such as Au or Pb or corrosion products (AgCl, $Cu_2O$). Consequently, the symbols close to the diagonal belong to slightly corroded or uncorroded pure Ag/Cu mixtures, while a symbol in the bottom left corner indicates an object rich in Au or Pb (as is the case for no. 897—which is actually not a coin, but a medallion). If this interpretation holds, one can likewise plot the sum of the copper-containing fractions against those containing silver, as shown in Figure 7 (b). Then, all symbols should be on or close to the diagonal unless other phases contribute to the bulk composition. Negative deviations from the diagonal indicate coins that were not made from pure Ag/Cu mixtures. In this way, Figure 7 (b) confirms in particular that all coins classified as HIM were typically composed of solely Ag and Cu in a wide range of ratios.

### NUMISMATIC DISCUSSION

Yule's metals identifications during the initial cataloguing for his Corpus (Yule in prep.) with the naked eye fared slightly worse than those of Munro-Hay (above): the former erred in the identification with 24 of the 99 analysed coins (25%). Deviations in Munro-Hay's identifications from our measured data result partly in the numismatic nomenclature that he uses (AR = silver, Æ = copper, B = billon, PB = lead). Copper and billon are the most difficult to discriminate from each other without the use of analytical methods. Debased silver alloyed with copper also poses difficulty. Silver may be difficult to identify with the naked eye because, to judge from our analyses, as little as 9% silver imparts a vaguely silvery colour. But coins that contain less than 50% of silver may be dark greyish and grainy in appearance. In the case of the Himyarite Raydan Series, which are usually silver coloured, the coin type may unconsciously influence the observer's visual identification of the metal, especially in the case of corroded examples. Close observation of the concave unworn reverse of such scyphates reveals traces of red oxidation that indicate the main metal (nos. 877, 879, 880 and 882). However, such traces do not guarantee copper metal (cf., e.g., no. 486, which contains 91% silver).

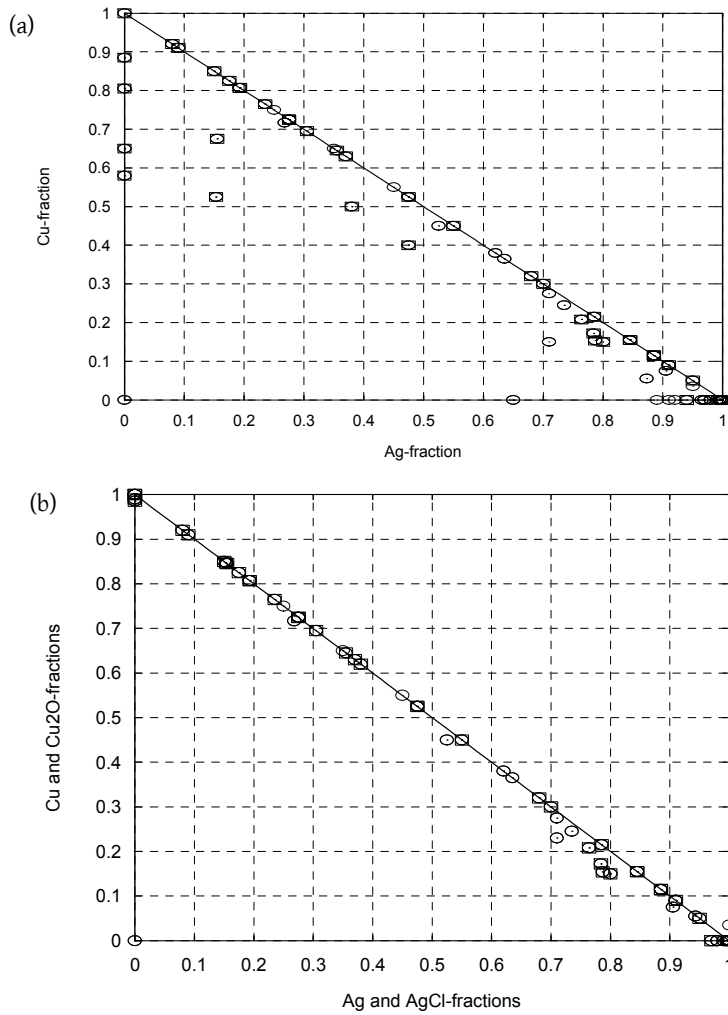*Non-destructive chemical analysis of Old South Arabian coins*



Figure 7 *SEL2: (a) Cu versus Ag phase fractions of all coins (ellipsoids) and Himyarite coins (rectangles). Note that the symbols on borders indicate coins of either Ag or Cu that are either corroded and/or contain additional phases such as Pb, Au or corrosion products (AgCl, $Cu_2O$). Consequently, symbols on diagonals indicate uncorroded pure (Ag, Cu) mixtures, while symbols close to the lower left corner represent specimens rich in Au or Pb. (b) Cu + Cu2O phase fractions versus Ag + AgCl phase fractions. Accordingly, all coins—and particularly HIM coins—are typically (Ag, Cu) mixtures of original compositions, as indicated in the diagram. Deviations from the diagonal indicate Pb admixtures.*

*A. Kirfel, W. Kockelmann and P. Yule*

Corrosion easily confounds optical identification. For example, the thick brown patina of no. 851 conceals a cast silver, not a copper Old Athenian Imitation, as one might conclude from the colour. The degree of corrosion can be estimated by comparing the densities of coins obtained from measurements (Table 2) with calculations on the basis of the phase fractions refined. Deviation between the measured and calculated values reveals corrosion—as, for example, in the case of no. 886, the corrosion of which is clear at a glance. On the other hand, coins that concur closely between calculated and measured values may also appear visually to be corroded (nos. 824, 831, 835 and 881) or clean (nos. 838 and 839).

In his catalogue of the collection of the State Ethnological Museum, Munro-Hay (2003, 207–8) identified six coins as forgeries with casting bubbles, poor form definition of the devices, no real use-wear and sometimes casting flanges from a bipartite mould. Corrosion of other Himyarite period coins in the same collection masks the bubbles. During our systematic photographic recording, we raised the number of such coins to 21: 92-316 292–297, 869–871, 873–883 and 890. Numbers 292 and 293 are cast from the same mould. While it seemed clear that except for cast Hadramitic coins, OSA coins are struck, now this proves always to be the rule.

Other anomalies occur: Coin no. 92-316 872 represents a unique example of two coins struck together, which Munro-Hay (2003) described as copper and lead. The neutron analysis shows, however, that it assays to 68% silver and 32% copper. Another anomalous example is 92-316 844 (Fig. 1, coin 3), which that author describes as 'plated silver on a copper alloy'. The neutron analysis yields 45% Ag and 55% Cu. Plating is not visible in our photos. The low-silver (15.3% Ag) struck coin no. 864 (Fig. 1, coin 4) comes into question as an ancient counterfeit for stylistic and iconographic reasons, since it also has no parallels.

The forgeries of Himyarite Raydan type that we analysed range in silver content from 8% (no. 875) to 80.3% (no. 296). Most lie at the lower end of the range, as shown in Table 2. Number 296 clearly shows the particular texture features of a cast coin (Fig. 5), but paradoxically has a high silver content (80.3%). Turning to all true and false low-silver coins of the Himyarite Raydan series, of the 19 assayed, 21 appear to be struck. Three other corroded struck coins consist of billon (92-316 886, 891; 93-316 487). Himyarite coinage and other rubrics in the visual arts are linked to developments in the Mediterranean (Yule 2007). Roman mints strike pure silver (>90%) until decline sets in during the third century ce (Göbl 1987). Despite the real regnal years, the alloying poses a potential reason to re-date OSA coins bearing the names of early kings, such as 'Amdān Bayyin Yuhaqbiḍ (reign ?100–120? CE; Fig. 1, coin 7) and as late as the devaluation of the Roman Severus (193–211 CE), at which time the silver content of the denarius decreased to 40–50% (Adkins 1998), marking the initial use of billon as a coinage metal.

In his catalogue of the collection of the State Ethnological Museum in Munich, Munro-Hay describes a hoard consisting of '249 coins of 'MDN BYN YNF, including six cast forgeries, 58 of 'MDN BYN, and nine Old Athenian Imitations, in fact 316 coins' (2003, 207–8). After our paper was accepted for publication, the previous owner of the State Ethnological Museum collection, Dr Werner Daum, explained to us that this published provenance for the coins rests on a misunderstanding. The source of the collection is not a hoard, but rather the collection of a diplomatic colleague.

Sixteen New Style Athenian Imitations (Fig. 1, coin 2) deviate with high AgCl values from the others in the State Museum collection and deserve comment. Such corrosion products might have arisen from emersion in sea water. These coins are also foreign to the others in terms of type. The provenance of these and of other coins in the collection is unclear. Probably, the New Style Athenian Imitations were purchased separately.

Which kind of OSA coins have the highest silver content? Having corrected the analysed fractions for oxidation products, we find three of the Bucranion series with an average silver content of 57%; 16 Old Style Athenian Imitations with 86.5%, 21 of the Himyarite Royal Raydan Series (excluding forgeries) with 88.0% and 16 New Style Athenian Imitations with 99.7% silver. Some coins with less than 50% silver were not used in the calculation of the averages, since the discussion centres on 'silver' coinage. Turning to Himyarite-period coins of a type normally struck in silver, the content varies greatly (68–100%), hindering an estimate of the silver content intended by the makers. One option is to distribute the coins of this type into a time when devaluation is suspected. The reverse of Figure 1, coin 6 brings to mind the angry look of the Roman emperor Caracalla (188–211 CE), which suggests a longer extension of the Raydan series than the regnal dates if this series, in this case of Karibʾīl Yuhanʿim. The New Style Athenian Imitations are practically pure silver at a time prior to silver devaluation—an intention, not a coincidence.

Coins of the Himyarite Raydan series appear in general to be better preserved than other OSA coins, an observation that is difficult to explain. The argument that they did not circulate as much as older coins is certainly questionable. The mean silver content is lower than for the New Style Athenian Imitations (88.02% versus 99.7%) and the fineness of the silver certainly is not the main factor in good preservation, as some believe.

### HIMYARITE COIN MANUFACTURE

The question of why Himyarite Raydan series scyphates (domed, convex or bowl-shaped) were produced remains unanswered. All of this series are scyphate, and vary in thickness from 0.07 to 0.27 mm for flattish coins and from 0.29 to 0.44 mm for pronounced scyphate ones. To judge from the collection under study, 23% of such coins are strongly scyphate. The relation between flat and highly convex coins amounts to 85.7% and 90.5% Ag—which can be taken as intentional, since the latter also show the finest-quality workmanship. The facial features are the best in OSA coinage, and details such as the hair are the finest. Most coins of the Raydan series are at least slightly scyphate: flattish (0.04–0.28 cm), 92-316 312, 92-316 751 120 and 92-316 859–863, 865–868; markedly scyphate (0.29–0.44 cm), 92-316 751 043, 053, 061, 063, 064, 068, 075, 92-316 887, 888, 889 and 93-317 488. The reason for the production of scyphates is not analogous to the devaluation of Byzantine coinage at the beginning of the 11th century (Weber 2003). Of the Raydan series, scyphates weigh the same as flat coins. Nor is there a reason to believe that scyphates result from a decrease in the Ag content and represent a measure to counter edge-splitting, as Moesta and Franke (1995) suggest for Byzantine scyphates. Without exception, those Himyarite scyphates tested are coins that are high in silver, and have no edge-splitting from the striking. The flatter ones show edge-splitting in a single case (no. 868). Moreover, scyphates of the Raydan series are more carefully struck than the flatter coins.

It seems likely that the flan of correct size and weight was first formed in dies into roughly the desired bowl-form, before the actual striking took place. Hamdani recounts that in his days in the Yemen, some 270 years after the demise of OSA, flans were first cast to the desired weight, and then further formed (curiously) by cold striking using water (Toll 1986). Notably, Hamdani's description of Himyarite coins reveals that 'The Himyar had on their coins the image of the sun, the moon and the planets (Athtar, h.b.s and Almaq or Yalmaq).' But in reality, such coins do not exist, and he repeats only hearsay, not what he himself actually saw. Probably, by high medieval times the production technology had changed. Numerous eccentric strikes show that the dies were not pegged to each other. But the strike is nearly always perfectly vertical. There is little

*A. Kirfel, W. Kockelmann and P. Yule*

evidence for a strike, repositioning and re-striking (reaffirming Bendall and Sellwood 1978). Since Hamdani's time, the flans have been hot-struck (idem, 38). Further research can seek traces of this method of manufacture for OSA coinage.

Except for cast Hadhrami coinage, OSA issues were struck probably by a single person, who held the upper die (the punch) in one hand and the hammer in the other. The lower die, or standard, may also have been mounted on a bench, to judge from a European medieval representation (Toll 1986). In antiquity, hot striking was fairly common, but whether or not it existed specifically in OSA coinage is unclear; the coins themselves do not reveal clear evidence for this or any other technique (cf. Grierson 1975; Weber 2003). The fact that, to date, no OSA coins from the same dies have been identified indicates that a huge number of the latter must have existed. Considering the ergonomic and technical considerations, scyphates were struck by means of a concave lower and convex upper die (Grierson 1975; Bendall and Sellwood 1978 (despite pp. 94–5, figs 1–4); Göbl 1987; Weber 2003). During striking, the obverse convexity of the coin lies face down, the reverse concavity face up. Upper dies wear out far more quickly than lower ones. On the other hand, in spite of faster wear on the upper die, the preservation of the concave face of the resulting coins is generally better than the obverse, which is caused by post-production use-wear and cannot be confused with wear of the dies.

## CONCLUSIONS

The usefulness of non-destructive neutron diffraction performed in both modes, angle- and energy-dispersive diffraction, is corroborated by application on selected pieces of Old South Arabian coinage. The selected objects constitute three main groups, Himyarite, New and Old Athenian Imitations, and a group of miscellaneous coins. The results obtained convey an idea of the potential, but also of the limitations of the neutron methods in numismatic research. With respect to compositions, HIM and IOA coins turned out to consist of the phases Ag and Cu, occasionally including some Pb, and the corrosion products cuprite and silver chloride. In contrast, the INA coins were made of pure silver and exhibited solely the corrosion product AgCl. In combination with experimental density determinations by gas-pycnometry, the chemical analyses were validated and supplemented by information about internal corrosion. Given the phase fractions of the main corrosion products, the initial composition of the coins at their time of production could be assessed. It was also shown that texture analyses can help to distinguish struck from cast material. As a further important result, the laboratory analyses of the metallic contents of our objects reveal the degree of error in subjective identifications of even experienced numismatists. This finding is not surprising, but adds further to the value of non-destructive neutron diffraction in the archaeological sciences. Thus, in summary, the data presented in this work can serve as a basis for future studies on the largely open question of when OSA coinage ends.

Although high-Ag New Athenian Imitation coins are early (i.e., late second century BCE to first century CE), the subsequent reduction of this metal in other OSA issues still cannot be proven to follow a simple diachronic pattern of devaluation—in no small part, a result of the lack of firm numismatic dating evidence.

## ACKNOWLEDGEMENTS

## REFERENCES

Adkins, R., 1998, *Handbook to life in ancient Rome*, Oxford University Press, Oxford.

Bendall, S., and Sellwood, D., 1978, The method of striking scyphate coins using two obverse dies, *Numismatic Chronicle*, **18**, 93–104.

Grave, P., Bird, R., and Potts, D. T., 1996, A trial PIXE/PIGME analysis of pre-Islamic Arabian coinage, *Arabian Archaeology and Epigraphy*, **7**, 75–81.

Göbl, R., 1987, *Numismatik Grundriss und wissenschaftliches System*, Battenberg, München.

Grierson, P., 1975, *Numismatics*, Oxford University Press, Oxford.

Hoover, O., and Huth, M., 2004, Rev. S. Munro-Hay, 2003, *American Numismatic Society*, **3**(2), 63–7.

Huth, M. (ed.), 2011, *Coinage of the caravan kingdoms* (in press).

Kirfel, A., Kockelmann, W., and Yule, P., 2006, Neutron diffraction analysis of silver coins from the Himyarite–Sabaean empire, in *Experimental reports of neutron scattering experiments at the FRJ-2 Reactor*, 75–6.

Kockelmann, W., Kirfel, A., and Hähnel, E., 2001, Non-destructive phase analysis of archaeological ceramics using TOF neutron diffraction, *Journal of Archaeological Science*, **28**, 213–22.

Kockelmann, W., Pantos, E., and Kirfel, A., 2000a, Neutron and synchrotron radiation studies of archaeological objects, in *Radiation in art and archaeometry* (eds. D. C. Creagh and D. A. Bradley), 347–77, Elsevier, Amsterdam.

Kockelmann, W., Weisser, M., Heinen, H., Kirfel, A., and Schäfer, W., 2000b, Application spectrum and data quality of the time-of-flight neutron diffractometer ROTAX at ISIS, *Materials Science Forum*, **321–4**, 332–7.

Kockelmann, W., Siano, S., Bartoli, L., Visser, D., Hallebeek, P., Traum, R., Linke, R., Schreiner, M., and Kirfel, A., 2006, Applications of TOF neutron diffraction in archaeometry, *Applied Physics A*, **83**, 175–82.

Larson, A. C., and von Dreele, R. B., 2004, *Los Alamos laboratory report LAUR no. 86-748*, Los Alamos, NM.

Moesta, H., and Franke, P., 1995, *Antike Metallurgie und Münzprägung*, Birkhäuser, Basel.

Munro-Hay, S., 2003, *Coinage of* Arabia Felix*: the pre-Islamic coinage of the Yemen*, Nomismata 5, Ed. Ennerre, Milan.

Rietveld, H.M., 1967, Line profiles of neutron powder diffraction peaks for structure refinement, *Acta Crystallographica*, **22**, 151–2.

Rietveld, H. M., 1969, A profile refinement method for nuclear and magnetic structures, *Journal of Applied Crystallography*, **2**, 65–71.

Rodriguez-Carvajal, J., 1993, Recent advances in magnetic structure determination by neutron powder diffraction, *Physica B*, **192**, 55–69.

Schäfer, W., Jansen, E., Skowronek, R., and Kirfel, A., 1997, The twin-diffractometer SV7 at the FRJ-2 as a workhorse for structure and texture research, *Physica B*, **234–6**, 1146–8.

Sedov, A., and Davidde, B., 1998, Das südarabische Münzwesen, in *Jemen: Kunst und Archäologie im Land der Königin von Saba'* (ed. W. Seipel), 195–9. Ausstellungskatalog Wien.

Toll, C., 1986, Kitab al-gauharatain al-'atiqatain al-ma'i'atain assafra wa'l-baida. Die beiden Edelmettalle Gold und Silber, Introduction, arabic text, and translation of al-Hamdani, 1968, *Die beiden Edelmetalle Gold und Silber* (ed. ACTA Univ. UPS), Studia Semitica UPS 1, Uppsala.

Young, R. A. (ed.), 1993, *The Rietveld method*, International Union of Crystallography/Oxford University Press, Oxford.

Yule, P., 2007, *Himyar-Spätantike im Yemen/Late Antique Yemen*, Linden Soft, Aichwald.

Yule, P., n.d., Corpus of Old South Arabian coins in European collections, in preparation.

Weber, K., 2003, Erkenntnisse zur Herstellung byzantinischer Elektrum-Skyphate, *Jahrbuch für Numismatik und Geldgeschichte*, **53–4**, 25–71.